Environ. Sci. Technol. **1998**, *32,* 3986−3992

Cyanide Destruction in Molten Carbonate Bath: Melt and Gas Analyses

M. ALAM* AND S. KAMATH

Department of Materials and Metallurgical Engineering, New Mexico Tech, Socorro, New Mexico 87801

Oxidation of combustible wastes in molten salt baths is being considered as an alternative to incineration. This paper examines the oxidation of cyanide ions (present in molten carbonate bath) by molecular oxygen as a function of the total gas mixture (O_2−Ar) flow rate, input gas composition (vol % O_2 in O_2−Ar mixtures), melt composition (initial mol % CN^- in CN^-−CO_3^{2-} baths), and melt temperature. The melts were sampled for the presence of CN^-, CNO^-, NO_2^-, and NO_3^- while the gas streams were sampled for N_2, N_2O, NO, NO_2, CO, and CO_2. While cyanide destruction proceeds rapidly (>90% loss of CN^- at 486 standard cm^3 per min, 40 vol % O_2, and 1243 K), NO_2 and CO emissions remain within the limits of air quality standards. Under all conditions CN^- and CNO^- were the major components, while NO_2^- and NO_3^- were the minor components of the melt. The amount of CNO^- present in the melt after any period of reaction was always smaller than the amount of CN^- lost from the melt during the same time period. The CO + CO_2 content of the gas was always much larger than the NO + NO_2 content. The CO/CO_2 ratio was always small while the NO/NO_2 ratio was always large. While N_2 content was larger than the NO + NO_2 content, no N_2O was ever detected. Material balance indicated that most of the nitrogen input to the system remained unaccounted after the reaction. Significance of the data are discussed.

Introduction

Cyanide-bearing compounds are used for a variety of manufacturing and processing operations. Under Code of Federal Regulations 40, part 261, the U.S. EPA designates a majority of these compounds as hazardous waste if they are discarded unused (*1*). These compounds are regulated as 'listed' wastes P and U (discarded commercial chemicals) because of their toxicity. Several of the P and U listed cyanide-bearing compounds may be destroyed by incineration to oxides of carbon and nitrogen along with moisture (*2*). One disadvantage of incineration is the high operating temperature (about 2300 K). At such high temperatures, and the fact that air is used for combustion in incinerators, there is also a potential for the formation of thermal NO_x (*3*). The oxides of carbon lead to green house effect (*4*), while the oxides of nitrogen lead to acid rain and cause ozone depletion (*5, 6*). The problems associated with some of these gases have prompted the U.S. EPA to restrict their release into the atmosphere (*7*). The exhaust gas streams from some incinerators, therefore, may need secondary processing (*4*), resulting in increased costs for an incinerator. There is a need for alternative processes that can effectively destroy the above-mentioned compounds without secondary processing of the exhaust gases. One such alternative is processing in a molten salt bath (*8*). The salt of choice is Na_2CO_3 because of its stability and nontoxicity at high temperatures, ability to retain acidic gaseous products, high thermal conductivity, availability, and cost. Mixtures of Na_2CO_3−Li_2CO_3−K_2CO_3, Na_2CO_3−NaCl, and Na_2CO_3−Na_2SO_4 have also been used (*9, 10*).

Processing in molten salt bath involves injecting a solid, liquid, or gaseous combustible waste into a molten salt bath along with air or oxygen. Organic carbon, nitrogen, fluorine, chlorine, sulfur, and phosphorus present in the waste are converted to carbonates, nitrites and nitrates, fluorides, chlorides, sulfites and sulfates, and phosphates, respectively, and retained in the melt. The exhaust gas streams contain moisture along with small quantities of CO, CO_2, N_2, N_2O, NO, NO_2, F_2, Cl_2, HF, HCl, SO_2, SO_3 and phosphorus-bearing gases, which can be released into the atmosphere without secondary processing. So far, this technology has been used to process a wide variety of organic and mixed wastes (*8*−*13*), and the results suggest that it could be a viable alternative to incineration. No data, however, has been obtained regarding the oxidation of cyanides in molten carbonate baths. Such data would be of interest in assessing the technical feasibility of this type of processing for the destruction of various cyanide compounds such as hydrogen cyanide, acetonitrile, acrylonitrile, propionitrile, methyl acrylonitrile, propane nitrile, methyl isocyanate, cyanogen, etc. The objective of this study was to understand the mechanism of oxidation of cyanide (NaCN) by reaction with oxygen in the presence of molten carbonate (Na_2CO_3).

Experimental Section

The chemicals used were ACS grade NaCN and anhydrous Na_2CO_3. A 50 g sample was prepared by mixing NaCN and Na_2CO_3 in desired proportions and transferred to an alumina crucible (9 cm high × 4 cm o.d.), which in turn was weighed and placed inside a one-end-closed cylindrical high-density alumina tube (45 cm high × 6 cm o.d.). The tube top was sealed with a rubber stopper that had openings for gas inlet and exhaust and thermocouple insertion. The top end of the gas inlet tube had a tee joint for argon and oxygen lines that were connected to rotameters for monitoring the gas flow rates. The gas inlet tube reached up to the top of the crucible to ensure that reactant gas impinged on the surface of the molten salt bath. The exhaust tube was also attached to a tee joint, one end of which was connected to a gas bubbler and subsequently to the exhaust vent while the other end served as the gas sampling port. The thermocouple was type K and was positioned between the inner wall of the reactor tube and the outer wall of the crucible. Temperature was monitored by a digital thermometer (Omega HH81). The entire assembly was placed in a vertical tube furnace (Lindberg Type 56622) that could be heated to 1473 K. The furnace temperature was regulated by a temperature controller (Omega 6100) to within ±4 K. Initially, the entire system was purged with argon gas (20 ppm impurities) flowing at 300 standard cm^3 for 45 min before the furnace was turned on. During preheating (preheating time varied between 48 and 56 min depending the desired temperature), argon flow was maintained at 300 standard cm^3 per min. Once the temperature reached the desired value and stabilized, the reaction was initiated by supplying an argon−oxygen gas mixture of known composition flowing at a

* To whom correspondence should be addressed. E-mail address: alam@nmt.edu; tel: (505)835-5831; fax: (505)835-5626.

10.1021/es9710969 CCC: $15.00
Published on Web 10/24/1998

TABLE 1. Possible Chemical Reactions of NaCN and Relevant Thermodynamic Data

reaction no.	reaction	ΔG° (kJ/mol CN^-)[a]	K_e at 1093 K
1	$CN^- + 1/2O_2 = CNO^-$	399.7 + 0.1486 T	2.2×10^{11}
2	$CN^- + 3/2O_2 = NO_2^- + CO$	−335.8 + 0.0493 T	2.9×10^{13}
3	$CN^- + 2/1O_2 = NO_2^- + CO_2$	−617.8 + 0.1358 T	2.7×10^{22}
4	$CN^- + 2/1O_2 = NO_3^- + CO$	−432.4 + 0.1350 T	4.1×10^{13}
5	$CN^- + 5/2O_2 = NO_3^- + CO_2$	−714.5 + 0.2215 T	3.8×10^{22}
6	$CN^- + 1/1O_2 = 1/2CO_3^{2-} + 1/2CO + 1/2N_2$	−519.4−0.0531 T	4.0×10^{27}
7	$CN^- + 5/4O_2 = 1/2CO_3^{2-} + 1/2CO + 1/2N_2O$	−477.4 + 0.0893 T	1.4×10^{18}
8	$CN^- + 3/2O_2 = 1/2CO_3^{2-} + 1/2CO + NO$	−428.8 + 0.0403 T	2.4×10^{18}
9	$CN^- + 2/1O_2 = 1/2CO_3^{2-} + 1/2CO + NO_2$	−487.1 + 0.1166 T	1.5×10^{17}
10	$CN^- + 5/4O_2 = 1/2CO_3^{2-} + 1/2CO_2 + 1/2N_2$	−660.4−0.0963 T	3.9×10^{36}
11	$CN^- + 3/2O_2 = 1/2CO_3^{2-} + 1/2CO_2 + 1/2N_2O$	−618.4 + 0.1326 T	4.2×10^{22}
12	$CN^- + 7/4O_2 = 1/2CO_3^{2-} + 1/2CO_2 + NO$	−570.0 + 0.0836 T	7.5×10^{22}
13	$CN^- + 9/4O_2 = 1/2CO_3^{2-} + 1/2CO_2 + NO_2$	−628.3 + 0.1600 T	4.7×10^{21}

[a] ΔG° is the standard free energy change of reaction at temperature T (K) and K_e is the equilibrium constant of the reaction.

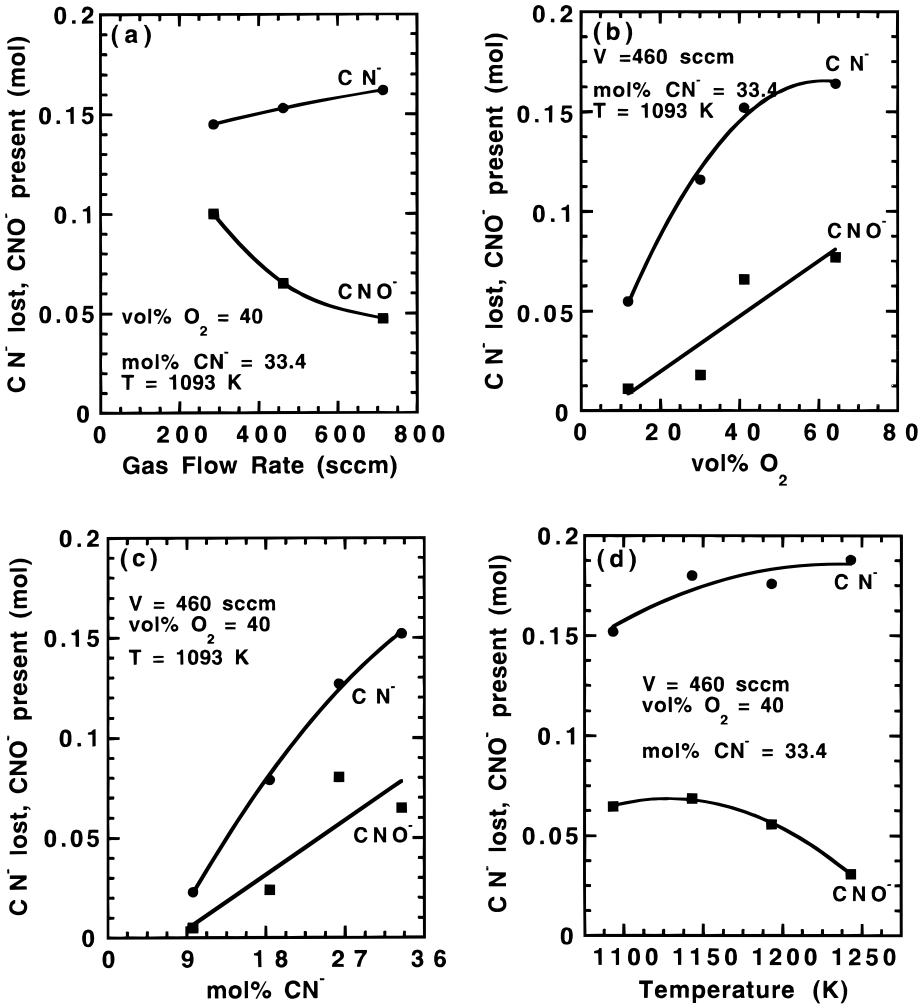

FIGURE 1. Amounts of CN^- lost from the melt and CNO^- present in the melt after 1 h of reaction as a function of (a) gas flow rate, (b) vol % O_2 in the input gas, (c) initial mol % CN^- in the melt, and (d) melt temperature. The variables kept constant during the experiments are also shown.

predetermined rate. Oxygen used was 99.6% pure. Five milliliter gas samples were withdrawn from the exhaust line using a gas-tight syringe at regular intervals after the initiation of the reaction for the duration of 1 h and collected in evacuated gas-tight plastic bags that were filled with 1 L of argon. At the end of 1 h, the reaction was terminated by stopping the oxygen flow and turning off the furnace. During cooling, argon continued to flow at 300 standard cm^3 per min. It took about 3 h to cool to room temperature, but temperature dropped below the melting point of carbonate within 3 min. Once the reactor cooled to room temperature, it was opened, and the crucible was withdrawn and weighed. The contents were then removed and crushed to give a uniform powder for analyses. The effects of four different processing variables were studied. These included $Ar-O_2$ reactant gas mixture flow rate (285−710 standard cm^3 per min), reactant gas composition (11.8−63 vol % O_2 in $Ar-O_2$ mixture), melt composition (9.7−33.4 mol % CN^- in $NaCN-Na_2CO_3$ mixture), and melt temperature (1093−1243 K). Although pure Na_2CO_3 melts at 1124 K, mixtures containing

TABLE 2. Possible Chemical Reactions of NaCNO

reaction no.	reaction
14	$CNO^- + 1/1O_2 = NO_2^- + CO$
15	$CNO^- + 3/2O_2 = NO_2^- + CO_2$
16	$CNO^- + 3/2O_2 = NO_3^- + CO$
17	$CNO^- + 2/1O_2 = NO_3^- + CO_2$
18	$CNO^- + 1/2O_2 = 1/2CO_3^{2-} + 1/2CO + 1/2N_2$
19	$CNO^- + 3/4O_2 = 1/2CO_3^{2-} + 1/2CO + 1/2N_2O$
20	$CNO^- + 1/1O_2 = 1/2CO_3^{2-} + 1/2CO + NO$
21	$CNO^- + 3/2O_2 = 1/2CO_3^{2-} + 1/2CO + NO_2$
22	$CNO^- + 3/4O_2 = 1/2CO_3^{2-} + 1/2CO_2 + 1/2N_2$
23	$CNO^- + 1/1O_2 = 1/2CO_3^{2-} + 1/2CO_2 + 1/2N_2O$
24	$CNO^- + 5/4O_2 = 1/2CO_3^{2-} + 1/2CO_2 + NO$
25	$CNO^- + 7/4O_2 = 1/2CO_3^{2-} + 1/2CO_2 + NO_2$

9.7−33.4 mol % NaCN (balance Na_2CO_3) are in the molten state in the mentioned temperature range (*14*).

The melts were analyzed for the presence of cyanide (CN^-), cyanate (CNO^-), nitrite (NO_2^-), and nitrate (NO_3^-) using the EPA Methods 9010, 4500 CN^-(L)/4500 NH_3(C), 4500 NO_2^-, and 4500 NO_3^-, respectively (*15*). The last three analyses involved colorimetry. The colorimeter used was Milton Roy Spectronic GENESYS 5 spectrophotometer. Standard solutions were always analyzed along with the samples for quality assurance. The gas samples were analyzed for the presence of N_2 (by a GowMac Series 550 gas chromatograph, equipped with a thermal conductivity detector), N_2O (by a Perkin-Elmer Model 1710 FTIR spectroscope), NO and NO_2 (by a Monitor Labs Inc. Model ML 9841A NO_x chemiluminescence analyzer), and CO and CO_2 (by a Liston Scientific Enviromax 3000 analyzer).

Results and Discussion

Possible Chemical Reactions of Cyanide. The reaction between molten NaCN (mixed with molten Na_2CO_3) and oxygen gas may result in the formation of cyanate (NaCNO), nitrite ($NaNO_2$), nitrate ($NaNO_3$), and carbonate (Na_2CO_3) in the liquid phase and N_2, N_2O, NO, NO_2, CO, and CO_2 in the gas phase. The relevant chemical reactions are presented in Table 1. To assess the feasibility of these reactions, the standard free energy changes of the reactions (in the 1093−1243 K temperature range) were calculated and are presented in Table 1. The standard free energy of formation data presented in refs *16* and *17* were used for this purpose. For NaCNO, the standard free energy of formation at different temperatures was estimated from the standard heat of formation, entropy, and heat capacity at 298 K (*18*). The corresponding equilibrium constants at 1093 K are also listed in Table 1. Large values of the equilibrium constants suggest that, at oxygen partial pressures used in this study, all the reactions are thermodynamically feasible.

Effects of the Processing Variables on Melt Composition. The melts were analyzed after 1 h of reaction for the presence of CN^-, CNO^-, NO_2^-, and NO_3^-. This reaction time was chosen because at the highest melt temperature of 1243 K, the cyanide loss reached about 90% of its original value after 1 h of reaction. The amount of cyanide lost from the melt and the amount of cyanate present in the melt after 1 h of processing are presented in Figure 1a−d as a function of the four processing variables. The smooth lines/curves are drawn for good representation of the data points and have no other significance. The amount of cyanate present in the melt after 1 h of processing results from a balance between the rate of formation of cyanate via reaction 1 (Table 1) and the rate of oxidation of cyanate via reactions 14−25 (Table 2). The amount of CNO^- present in the melt is always smaller than the amount of CN^- lost during reaction. This result is indicative of two possibilities. First, beside forming CNO^-, CN^- may also form NO_2^-, NO_3^-, and CO_3^{2-} via reactions 2−13 (Table 1) resulting in more cyanide loss and less cyanate in the melt as observed. The melt analyses indicate the presence of very small amounts of NO_2^- and NO_3^-, and CO_3^{2-} analysis was not performed. The presence of very small amounts of NO_2^- and NO_3^- however is not sufficient evidence to rule out the importance of their formation because nitrite and nitrate may evaporate from the melt during the course of the reaction. $NaNO_2$ melts at 557 K and begins to volatilize significantly above 593 K, while $NaNO_3$ melts at 582 K and begins to volatilize significantly above 773 K (*19*). These temperatures are well below the lowest processing temperature of 1093 K. Second, CNO^- may oxidize to NO_2^-, NO_3^-, and CO_3^{2-} resulting in less cyanate in the melt as observed. It is very likely that both possibilities exist.

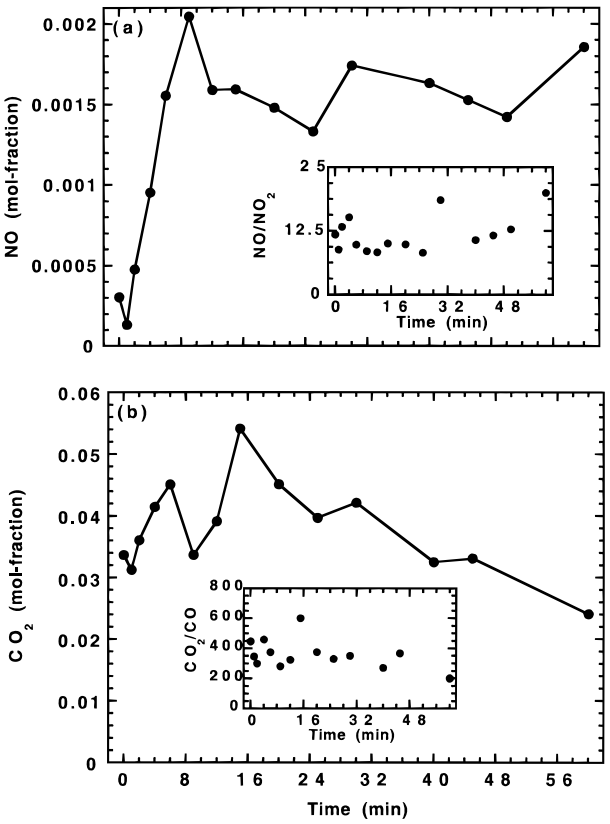

FIGURE 2. Exhaust gas composition as a function of time: (a) NO and (b) CO_2. Insets indicate the variation of the NO/NO_2 and CO_2/CO ratios (gas flow rate = 460 standard cm^3 per min, vol % O_2 in the input gas = 40, initial mol % CN^- in the melt = 18.4, melt temperature = 1093 K).

The data in Figure 1a−d indicate that both the amount of cyanide lost from the melt and the amount of cyanate left in the melt increase with increasing oxygen content of the input gas (due to the availability of more oxygen for fixed amount of cyanide) and with increasing initial cyanide content of the melt (due to the availability of more cyanide for fixed amount of oxygen input). The effects of the initial gas flow rate and the melt temperature are quite different. With increasing gas flow rate and temperature, the amount of cyanide lost from the melt increases (expected due to increased agitation of the bath leading to better reactant contact and due to faster reaction kinetics, respectively), but the amount of cyanate present in the melt decreases (probably due to higher rate of oxidation of cyanate via reactions 14−25 as compared to the rate of oxidation of cyanide via reaction 1).

Time Evolution of the Exhaust Gas Composition. The gas phase was analyzed for N_2, N_2O, NO, NO_2, CO, and CO_2.

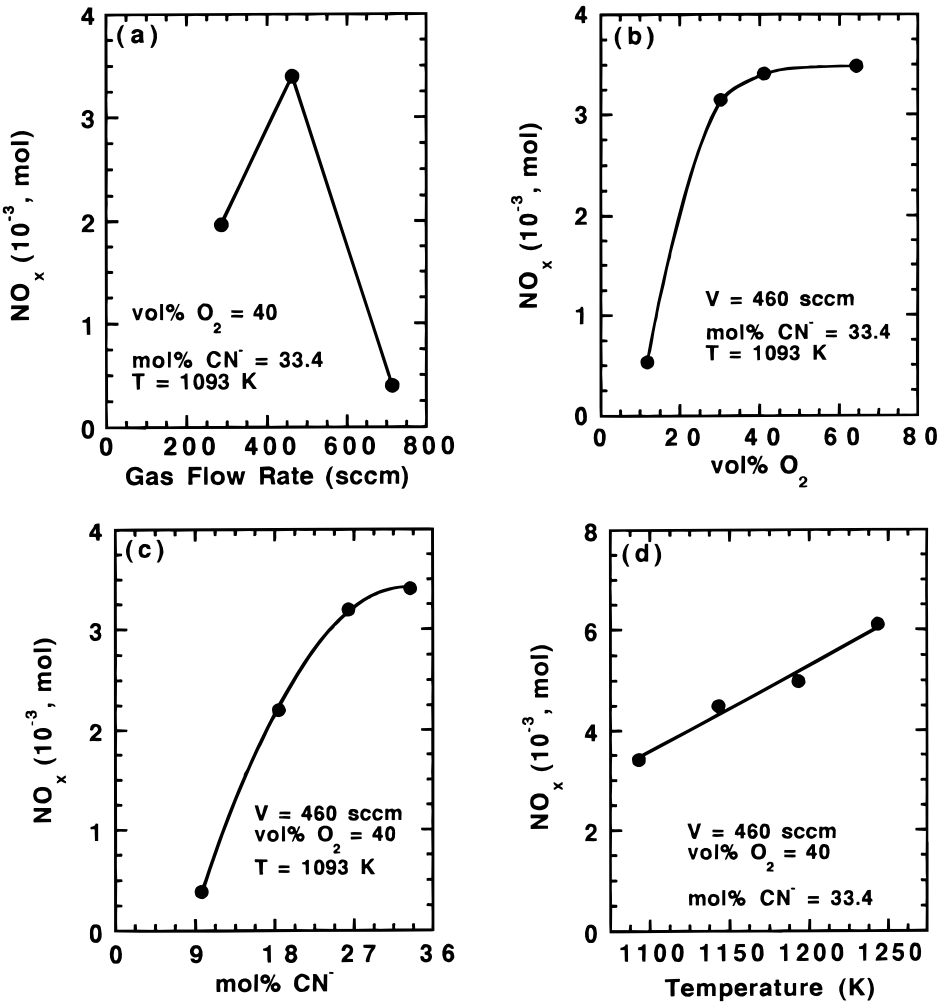

FIGURE 3. Effect of the process variables on the production of NO_x: (a) gas flow rate, (b) vol % O_2 in the input gas, (c) initial mol % CN^- in the melt, and (d) melt temperature. The variables kept constant during the experiments are also shown.

Typical plots of the concentrations of NO and CO_2 as a function of time are shown in Figure 2a,b. In all cases, the NO and CO_2 contents increased initially with time followed by either a nearly constant NO and CO_2 content for the duration of the reaction (indicating the establishment of steady state) or an erratic behavior that did not seem to follow any trend. This erratic behavior is attributed to the buildup of pressure inside the reactor tube due to evaporation of materials and their subsequent condensation in the exhaust line. To minimize the problem, the exhaust line was cleaned before the start of each experiment. In all cases, the CO_2 content in exhaust gas was significantly higher than the NO content. The insets in Figure 2a,b indicate the variations of the NO/NO_2 and the CO_2/CO ratios, respectively, as a function of time. The NO and the CO_2 contents are significantly higher than the NO_2 and the CO contents, respectively. This was true in all cases; however, the ratios changed slightly with changes in the processing variables. The average NO/NO_2 and CO_2/CO ratios during 1 h of reaction are 11.8 and 359, respectively. The corresponding equilibrium values of the ratios calculated from the available thermodynamic data (*16*) and at oxygen partial pressure of 0.4 atm are 24.4 and 6×10^8, respectively, at 1093 K, and 9×10^{-7} and 5×10^{44}, respectively, at room temperature.

Effects of the Variables on the Amounts of NO, NO_2, CO, and CO_2. The total amounts of NO_x ($NO + NO_2$) and CO_x ($CO + CO_2$) produced during the 1 h reaction period (in moles) were obtained from the knowledge of the areas under the NO, NO_2, CO, and CO_2 plots and the gas law. Effects of the process variables on the amounts of NO_x and CO_x are shown in Figures 3a–d and 4a–c, respectively. Figure 3a indicates that, with increasing gas flow rate, the amount of NO_x produced increases at first and then decreases. With increasing gas flow rate, more cyanide is lost and less cyanate is left in the melt (see Figure 1a), suggesting that reactions 1, 8, 9, 12, 13, 20, 21, 24, and 25 are taking place. These reactions (except reaction 1) should lead to higher amounts of NO_x in the gas phase with increasing gas flow rate (due to more oxygen input and excessive agitation of the reaction bath) as observed. The decrease in the amount of NO_x produced at high gas flow rate can be attributed to at least two factors. First, beyond a total gas flow rate of 460 standard cm^3 per min, the melt becomes saturated with oxygen, and production of NO_x levels off. Further increase in the gas flow rate results in dilution of the exhaust gas stream resulting in lower concentration of NO_x. Low levels of NO_x lead to lowering of the amount of NO_x produced during the 1 h reaction period. Second, at high gas flow rate, enough NO and NO_2 may exist in the system for the following reactions to occur:

$$CO_3^{2-} + 2NO \leftrightarrow 2NO_2^- + CO \quad (26)$$

$$CO_3^{2-} + 2NO_2 \leftrightarrow 2NO_3^- + CO \quad (27)$$

$$CO_3^{2-} + 2NO_2 \leftrightarrow NO_2^- + NO_3^- + CO_2 \quad (28)$$

Reactions 26–28 would lead to a decrease in the amount of

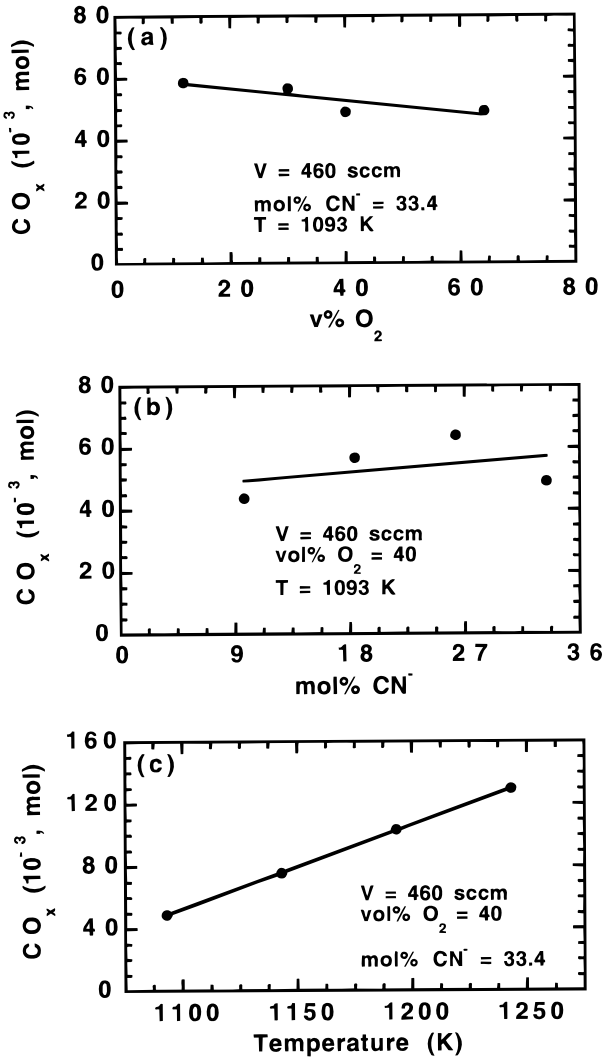

FIGURE 4. Effect of the process variables on the production of CO_x: (a) vol % O_2 in the input gas, (b) mol % CN^- in the melt, and (c) melt temperature. The variables kept constant during the experiments are also shown.

NO_x with a concomitant increase in the amount of CO_x. Unfortunately, CO_x data were not collected as a function of the gas flow rate. These reactions are in agreement with the findings of a previous study where it was pointed out that the melt accumulates nitrogen compounds when CO and CO_2 levels are low and releases nitrogen oxides when CO and CO_2 levels are high (*10*).

Figures 3b and 4a indicate that the amount of NO_x increases (rapidly at first and then slowly) and the amount of CO_x decreases (slowly), respectively, with increasing oxygen content of the input gas. The increase in the amount of NO_x is due to the availability of more oxygen in the system that causes reactions 8, 9, 12, 13, 20, 21, 24, and 25 to take place. The leveling off of the NO_x is probably due to the fact that the melt becomes saturated with oxygen. These reactions should also lead to the production of more CO_x in the gas phase. However, Figure 4a indicates a slight decrease in the amount of CO_x as oxygen content of the input gas increases. Given that the observed decrease is very small, experimental errors might explain the observation for CO_x. Figures 3c and 4b indicate that the amounts of NO_x and CO_x increase with increasing initial cyanide content of the melt. The increases are due to the availability of more cyanide in the system that causes reactions 8, 9, 12, 13, 20, 21, 24, and 25 to occur. The increases in the amounts of NO_x and CO_x for a given increase in the mole % CN^- are however different. Figures 3d and 4c indicate that the amounts of NO_x and CO_x increase with increasing temperatures. The increases are attributed to the higher rates of reactions 8, 9, 12, 13, 20, 21, 24, and 25. The increases in the amounts of NO_x and CO_x for a given increase in the temperature are however different.

Nitrogen Balances. Nitrogen balances were performed by considering nitrogen input into the system as CN^- and nitrogen output from the system as CN^-, CNO^-, NO_2^-, NO_3^-, and NO_x ($NO + NO_2$) in moles. The balances are shown in Table 3. Under all operating conditions, the amount of nitrogen input is significantly higher than the amount of nitrogen output. The discrepancy varies between 22 and 78% with the highest discrepancy at the highest temperature. No N_2O was ever detected in the gas phase, but one sample analyzed for N_2 showed about 0.8 mol % N_2. Assuming this value to represent the average concentration of N_2 in the gas phase during the 1 h reaction period, the amount of N_2 produced during the course of the reaction was calculated to be 15 mmol. Perusal of Table 3 indicates this value to be 2.5−38.5 times higher than the total amount of NO_x produced (depending on the processing conditions) during the same time period, suggesting the importance of reactions involving the liberation of N_2. In any case, even if such reactions are considered, the system nitrogen balances are not likely to change in any significant manner. It is believed that the main source of discrepancy in nitrogen balance is the loss of nitrogen-bearing species such as NaCN and NaCNO and particularly $NaNO_2$ and $NaNO_3$ from the melt via evaporation during the course of reaction. These materials subsequently condensed in cooler regions of the reactor and the exhaust gas line and remained unaccounted. This phenomena could also explain the higher discrepancies at higher melt temperatures where evaporation becomes even more important.

Discussions and Applicability

The data indicate cyanide and cyanate to be the dominant species in the melt and N_2 (based on one measurement), NO, and CO_2 to be the dominant species in the gas phase. Minor components of the melt are NO_2^- and NO_3^-, and those of the gas phase are NO_2 and CO. The NO content is always substantially lower than the CO_2 content. It can therefore be concluded that the dominant chemical reactions occurring in the system are 1, 3, 5, 10, 15, 17, and 22. The presence of some NO_x (nitrogen balance indicates that NO_x content of the gas varies between 0.2 and 3.2% of the cyanide input) suggests the importance of reactions 12 and 24. Since the data indicate significantly more CO_2 than NO in the gas phase, reactions 12 and 24 are considered minor. The reactions involving the consumption of NO and the production of CO_2 (reactions 26−28) cannot be ignored. The presence of small amounts of NO_2 and CO in the gas phase suggest that reactions 2, 4, 6, 8, 9, 13, 14, 16, 18, 20, 21, and 25 also occur to some extent. The reactions among the various gaseous species have not been considered. Some of these reactions include the following:

$$CO + 1/2O_2 \leftrightarrow CO_2 \quad (29)$$

$$NO + 1/2O_2 \leftrightarrow NO_2 \quad (30)$$

$$NO \leftrightarrow 1/2N_2 + 1/2O_2 \quad (31)$$

$$NO_2 \leftrightarrow 1/2N_2 + O_2 \quad (32)$$

Reactions 29 and 30 should be very important in determining the CO/CO_2 and the NO/NO_2 ratios in the sampled gases. In the temperature range of interest, the standard free energy changes associated with reactions 31 and 32 are large and negative. This suggests that NO and NO_2 might be intermediates in N_2 formation.

TABLE 3. Nitrogen Balances

variable	n^i (CN^-) (mol)	n° (CN^-) (mol)	n° (CNO^-) (mol)	n° (NO_2^-) (mmol)	n° (NO_3^-) (mmol)	n° (NO_x) (mmol)	n° (total) (mol)	% Δ[a]
V (standard cm^3 per min)								
285	0.192	0.047	0.100	0.049	0.220	1.97	0.149	22.4
460	0.192	0.040	0.065	0.009	0.245	3.41	0.109	43.2
706	0.192	0.030	0.048	0.001	0.107	0.40	0.079	58.9
vol % O_2								
11.8	0.192	0.137	0.011	0.141	0.563	0.53	0.149	22.4
30.2	0.192	0.076	0.018	0.113	0.552	3.15	0.098	50.0
40.0	0.192	0.040	0.065	0.009	0.245	3.41	0.109	43.2
64.2	0.192	0.028	0.077	0.008	0.212	3.49	0.109	43.2
mol % CN^-								
9.7	0.048	0.025	0.005	0.105	0.009	0.39	0.031	35.4
18.4	0.096	0.017	0.024	0.150	0.200	2.21	0.044	54.2
26.3	0.144	0.017	0.081	0.007	0.178	3.20	0.101	29.9
33.4	0.192	0.040	0.065	0.009	0.245	3.41	0.109	43.2
T (K)								
1093	0.192	0.040	0.065	0.009	0.245	3.41	0.109	43.2
1143	0.192	0.012	0.069	0.007	0.418	4.50	0.086	55.2
1193	0.192	0.016	0.056	0.006	0.226	5.00	0.077	59.9
1243	0.192	0.004	0.031	0.133	0.082	6.11	0.041	78.6

[a] % Δ represents percent of input nitrogen that remains unaccounted.

Preliminary kinetic measurements indicate the rate of loss of cyanide from the melt (in wt % CN^-/s) to increase with increase in the value of each variable. The reader can develop some feel for the process kinetics by considering the fact that a sample containing 10 wt % CN^- upon reaction (with $Ar-O_2$ gas mixture containing 40 vol % O_2, flowing at a rate of 486 standard cm^3 per min, and at 1243 K) lost more than 90% of the initial CN^- in about 30 min.

The Federal Clean Air Act of 1990 has put severe constraints on the operators of waste processing facilities to restrict the emissions of undesirable gases into the ambient environment. Presently, no standards exist regarding the NO_2 and CO emissions from molten salt bath reactors used for treatment of hazardous wastes. Therefore, it is difficult to speculate on the magnitude of emissions from such reactors. The current ambient air quality standards for NO_2 and CO are 0.053 ppm by volume (annual average concentration) and 9 ppm by volume (8 h average concentration) or 35 ppm by volume (1 h average concentration), respectively (*20*). Similarly, the emission standards for NO_x and CO at large municipal waste combustion (MWC) plants are 180−230 ppm by volume (daily average basis) and 50−200 ppm by volume (4−24 h average basis), respectively (*21*). Clearly minimization of NO_x and CO in the emissions is desirable. The EPA's proposed emission standards for MWC can, however, serve as a basis upon which to compare the NO_x and CO emissions from the molten salt reactors used for the combustion of hazardous wastes. For the oxidation of CN^- by O_2 in molten CO_3^{2-} bath, this study indicates the NO_2 and CO emissions to be about 180 and 115 ppm, respectively (1 h average). These numbers are within the limits of emission air quality standards. There is even further potential of reducing the emissions by manipulating the processing parameters. The NO_x and CO contents of the emissions are functions of the amount of air supplied per unit amount of fuel and temperature. Both the NO_x and the CO content increase with increasing temperature (*22*). Thus, operating the molten salt reactor at lower temperatures has real merit in terms of compliance of the process with regard to emission quality standards. The use of low-temperature eutectic mixture of Li−Na−K carbonates is very promising in this regard.

The development of molten salt processing technology is likely to assist in the destruction of a wide variety of wastes. Some potential wastes include chemical warfare agents (mustard gas), munitions (TNT), chemical wastes (PCBs), pesticides (DDT), combustible wastes from nuclear power plants (tributyl phosphate), etc. Hazardous wastes containing cyanide constituents are generated from specific industrial sources such as production of inorganic chemicals and pigments, ink formulations, etc. Salts of various cyanide complexes are listed as discreet chemical constituents of discarded chemical products, off-specification species, container residues, etc. Studies of cyanide destruction in molten salt bath will benefit these manufacturing operations.

Acknowledgments

The research on which this paper is based was funded in part by the U.S. Department of Energy through the New Mexico Waste-management Education & Research Consortium (WERC).

Supporting Information Available

Additional experimental details and discussion (2 pages). Ordering information is given on any current masthead page.

Literature Cited

(1) *Code of Federal Regulations 40, Part 261*; U.S. Government Printing Office: Washington, DC, 1995, pp 31−33.

(2) Grosse, D. W. *J. Air Pollut. Control Assoc.* **1986**, *36*, 603.

(3) Seinfeld, J. H. *Atmospheric Chemistry and Physics of Air Pollution*; John Wiley and Sons: New York, 1986; pp 80−85.

(4) Rubel, F. N. *Incineration of Solid Wastes*; Noyes Data Corporation: Park Ridge, NJ, 1974; pp 3−48.

(5) Cudby, E. E. In *Air Pollution and Their Effects on the Terrestrial Ecosystem*; Legge, A. H., Krupa, S. V., Eds.; John Wiley and Sons: New York, 1986; pp 15−39.

(6) Hulgaard, T.; Dam-Johansen, K. *Environ. Prog.* **1992**, *11*, 302.

(7) Demerjian, K. L. In *Air Pollution and Their Effects on the Terrestrial Ecosystem*; Legge, A. H., Krupa, S. V., Eds.; John Wiley and Sons: New York, 1986; pp 105−124.

(8) McKenzie, E.; Grantham, L. F.; Richards, L. F.; Paulson, R. B. *AIChE Symp. Ser.* **1976**, *No. 154*, 69.

(9) Watkins, B. E.; Upadhye, R. S.; Pruneda, C. O.; Brummond, B. A. *Emissions from Energetic Materials Waste During the Molten Salt Destruction Process*; Lawrence Livermore National Laboratory Report E 1.99:UCRL-JC-117576; 1994.

(10) Haas, P. A.; Rudolph, J. C.; Bell, J. T. *Molten Salt Oxidation of Mixed Wastes—Preliminary Bench Scale Experiments without Radioactivity*; Oak Ridge National Laboratory Report E 1.99: ORNL/TM-12765; 1994.

(11) Yosim, S. J.; Kellog, L. G.; Sudar, S. *Molten Salt Destruction of HCB and Chlordane—Bench and Pilot Scale Tests*; Industrial Environment Research Laboratory; U.S. EPA Report EP 1.89/2:600/s 2-84-148; 1984.
(12) Upadhye, R. S.; Wilder, J. G. *Molten Salt Destruction of Rubber and Chlorinated Solvents*; Lawrence Livermore National Laboratory Report E 1.99:UCRL-JC-117575; 1994.
(13) Rudolph, J. C.; Haas, P. A.; Bell, J. T. *Molten Salt Oxidation of Chloro-Organic Compounds: Experimental Results for Product Gas Composition and Final Studies*; Oak Ridge National Laboratory Report E 1.99:ORNL/TM-12941; 1995.
(14) Levin, E. M.; Robbins, C. R.; McMurdie, H. F. *Phase Diagram for Ceramists*; The Americam Ceramic Society: Columbus, OH, 1964; p 513.
(15) *Standard Methods for the Examination of Water and Wastewater*, 18th ed.; Greenberg, A. E., Clesceri, L. S., Eaton, A. D., Franson, M. A. H., Eds.; American Public Health Association: Washington, DC, 1992; pp 4-23, 4-33, 4-78, 4-85, 4-87.
(16) *JANAF Thermochemical Tables*, 3rd ed.; Chase, M. W., Jr., Davies, C. A., Downey, J. R., Jr., Frurip, D. J., McDonald, R. A., Syverud, A. N., Eds.; ACS/AIP/USNBS: NewYork, 1985.
(17) Barin, I. *Thermochemical Data of Pure Substances*, 2nd ed.; VCH: New York, 1993; p 982.
(18) Wagman, D. D.; Evans, W. H.; Parker, V. B.; Schumm, R. H.; Nuttall, R. L. *Selected Values of Chemical Thermodynamic Properties*; U.S. Department of Commerce/NBS Technical Note 270-8; U.S. Government Printing Office: Washington, DC, 1981; p 24.
(19) *Lange's Handbook of Chemistry*, 14th ed.; Dean, J. A., Ed.; McGraw-Hill: New York, 1992; p 3.51.
(20) *Code of Federal Regulations 40, Part 50*; U.S. Government Printing Office: Washington, DC, 1997; pp 7−8.
(21) *Code of Federal Regulations 40, Part 60*; U.S. Government Printing Office: Washington, DC, 1997; pp 67−70.
(22) Brunner, C. R. *Handbook of Incineration Systems*; McGraw-Hill, Inc.: New York, 1991; pp 7.7−7.14.

Received for review December 18, 1997. Revised manuscript received September 10, 1998. Accepted September 17, 1998.

ES9710969